aval Research Laboratory
hington, DC 20375-5000

NRL Memorandum Report 6738

Phase-Coded Waveforms and Range Superresolution

W. F. GABRIEL*

Radar Analysis Branch
Radar Division

**SFA, Inc.,*
Landover, MD 20785

November 5, 1990

REPORT DOCUMENTATION PAGE

Form Approved
OMB No. 0704-0188

1. AGENCY USE ONLY (Leave blank)	2. REPORT DATE	3. REPORT TYPE AND DATES COVERED
	1990 November 5	Interim Oct. 1989-Oct. 1990

4. TITLE AND SUBTITLE

Phase-Coded Waveforms and Range Superresolution

5. FUNDING NUMBERS

SEATASK 90-315

6. AUTHOR(S)

W. F. GABRIEL*

7. PERFORMING ORGANIZATION NAME(S) AND ADDRESS(ES)

Naval Research Laboratory
Washington, D.C. 20375-5000

8. PERFORMING ORGANIZATION REPORT NUMBER

NRL Memorandum
Report 6738

9. SPONSORING/MONITORING AGENCY NAME(S) AND ADDRESS(ES)

NAVSEA #PMS-400 B331 (R. Rogers)

10. SPONSORING/MONITORING AGENCY REPORT NUMBER

11. SUPPLEMENTARY NOTES

*SFA, Inc., Landover, MD 20785

12a. DISTRIBUTION/AVAILABILITY STATEMENT

Approved for public release; distribution unlimited

12b. DISTRIBUTION CODE

13. ABSTRACT *(Maximum 200 words)*

Phase-coded pulse-compression waveforms have been investigated for compatibility with superresolution processing techniques in the range domain. Two waveforms were tested via simulated data; a binary Barker code, and a quadriphase code. The binary code was not compatible and did not permit resolution finer than the conventional matched filter. The quadriphase code, on the other hand, was found to be partially compatible and permitted accurate resolution/location of one or two point-targets within a rangebin. However, it could not handle more than two closely spaced targets because of its inherent limitation of two degrees-of-freedom (for superresolution processing purposes). Therefore, these phase-coded waveforms are not recommended for high resolution processing in range. The processor burden would not be cost effective for the limited benefits available.

14. SUBJECT TERMS	15. NUMBER OF PAGES
Phase Coded Waveforms, Adaptive pulse compression, Range Superresolution	23
	16. PRICE CODE

17. SECURITY CLASSIFICATION OF REPORT	18. SECURITY CLASSIFICATION OF THIS PAGE	19. SECURITY CLASSIFICATION OF ABSTRACT	20. LIMITATION OF ABSTRACT
UNCLASSIFIED	UNCLASSIFIED	UNCLASSIFIED	SAR

CONTENTS

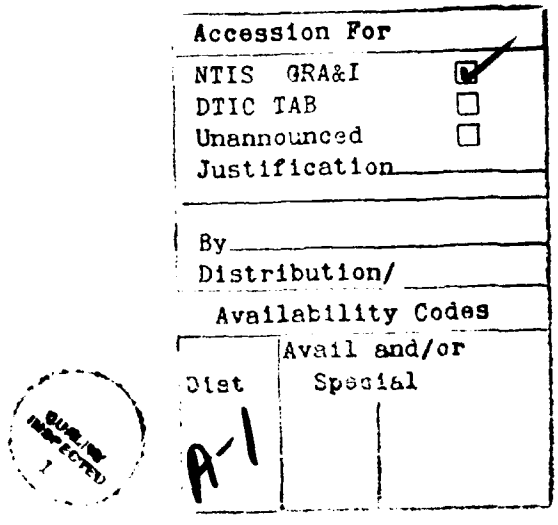

PHASE-CODED WAVEFORMS AND RANGE SUPERRESOLUTION

INTRODUCTION

A discussion of the general principles involved in achieving superresolution in the range domain is presented in reference [1], utilizing a linear FM chirp for the pulse compression waveform. There, it is pointed out that a crucial requirement is to have enough samplings (observation time) to permit decorrelation of multiple point-targets within a rangebin (analogous to multiple sources within a beamwidth in the spatial domain). In essence, we seek a uniform distribution of the scatterer phase data, as if they were sources of random phase signals. There are several ways in which the necessary decorrelation might be achieved, or at least approximated:

a. A slowly rotating object wherein the scatterers have sufficient doppler differences. This is a classic ISAR situation [2].

b. An object in straight-line motion (non-radial) wherein an equivalent rotation occurs over the observation time.

c. A stepped linear FM carrier shift (small increment per prf) which produces sufficient phase changes between scatterers spaced closely in range. This borrows from the classic linear FM ranging method [2,3].

Manuscript approved September 10, 1990.

d. Random frequency hopping of the carrier per prf to produce sufficient phase changes for small range separations.

e. Combinations of the above.

In addition to the decorrelation requirement, it also is necessary that the pulse compression waveform incorporate a phase differential which varies as a function of subpulse position (Again, analogous to spatial domain array phasing from sources within a beamwidth). This second requirement is readily satisfied by a linear FM chirp waveform, wherein the phase is a quadratic function.

Appendix A provides a brief review/analysis of the basic waveform signal data model from which one can compute superresolution in the range domain [1]. This processing was employed to generate the range estimate plots contained herein.

PHASE-CODED WAVEFORMS

Phase-coded waveforms have constituted an important class of signal for pulse-compression radar systems [3] because of their desirable transmitter power characteristics and the simplicity of associated transmitter/receiver implementations. Thus, it was

natural to investigate their compatibility with high-resolution data processing techniques. Phase-coded waveforms differ from FM chirp waveforms in that the long pulse is subdivided into a number of shorter subpulses. The subpulses are of equal time duration, each is transmitted with a particular phase, and the phase is selected in accordance with a phase code.

The most widely used type of phase coding is binary coding wherein the phase of the transmitted signal alternates between 0 and 180 degrees in accordance with a sequence of +1's and -1's. A special class of binary codes, known as Barker codes [4] are given in Table 1. Barker codes are optimum in the sense that the

TABLE 1 BARKER CODES

Length of Code N	Code elements	Peak-sidelobe ratio, db (-20 log N)
2	+-,++	- 6.0
3	++-	- 9.5
4	++-+,+++-	-12.0
5	+++-+	-14.0
7	+++--+-	-16.9
11	+++---+--+-	-20.8
13	+++++--++-+-+	-22.3

peak of the autocorrelation function is N, where N is the number of elements or length of the code, and the time-sidelobe magnitudes are unity or less. The Barker code of length N = 13 is the particular code utilized in the simulation waveform examples contained in this report, and Fig. 1 illustrates a conceptual schematic implementation for generating this waveform.

A quadriphase code [5,6] is one whose subpulses are phased in one of four states: 0, 90, 180, or 270 degrees. For our simulations, a restricted subset is employed wherein the subpulses feature a half-cosine shape and a phase change between adjacent subpulses of either +90 or -90 degrees. These restrictions create a constant amplitude pulse except for the leading and trailing edges, and eliminate phase transients which cause "spectral splatter." The quadriphase code described here is derived from a prototype biphase code, a Barker code of length N = 13, via the following transformation,

$$W_n = j^{(n-1)} e^{j\frac{\pi}{2}(B_n-1)} \qquad (1)$$

where W_n = quadriphase code complex number

B_n = biphase code integers

n = subpulse index

upon substituting for B_n the code values from Table 1, the following quadriphase code values are obtained for W_n;

$$\begin{aligned} n &= 1,\ 2,\ 3,\ 4,\ 5,\ 6,\ 7,\ 8,\ 9,10,11,12,13 \\ W_n &= +1,+j,-1,-j,+1,-j,+1,-j,+1,-j,-1,+j,+1 \end{aligned} \tag{2}$$

Figure 2 illustrates a conceptual schematic implementation for generating this waveform, utilizing the half-cosine subpulse. Note the in-phase and quadrature components, the overall constant amplitude (except for leading and trailing edges), and the slopes in the phase function, $\psi(t)$. This waveform actually extends over 15 rangebins even though it is based upon a Barker code of length 13, because of the half-cosine leading and trailing edges.

Another way of looking at the waveform is that the linearly changing phase shifts allow two frequencies during the encoded portion of the pulse; these are given by the center frequency, f_o, + and $-\Delta f$, where

$$\Delta f = \frac{\textit{phase shift per bit (part of cycle)}}{\textit{bit length (seconds)}}. \tag{3}$$

Such a modulation is similar to frequency shift keying [6]. Each frequency is tantamount to a degree-of-freedom for superresolution processing purposes.

SIMULATED DATA RESULTS

Data samples were generated [1] for radar scenarios involving one or more point targets located within a rangebin, using the above described phase-coded waveforms. Figure 3 illustrates the range estimate plots computed for a single 10 dB target from binary Barker code data, utilizing three different processing algorithms:

a. Fourier (matched filter response)
b. Capon's MLM algorithm
c. MUSIC eigenvector algorithm

These algorithms are described in reference [1]. It is evident in Fig. 3 that the two superresolution algorithms cannot function properly with bi-phase coded data and that this resolution performance is no better than the conventional matched filter. The technical reason for this behavior is that the simple binary phase codes maintain the same phase differential (bin to bin) regardless of the position of a target within a rangebin. Thus, there is no phase discriminant within a rangebin and the range estimates are limited to the conventional subpulse width.

The same single 10 dB target situation was then computed for the quadriphase code waveform described above, and Fig. 4 illustrates the range estimate plots for the same three

algorithms. Here we see that the quadriphase waveform data works well on a single target and correctly locates its position in range, within its particular rangebin.

Next, the quadriphase code waveform was used against two 10 dB targets located within the same rangebin, wherein the target separation is only 1/2 rangebin. Figure 5 illustrates the performance results, and we note that the conventional matched filter (Fig. 5 (a)) is unable to resolve the two closely spaced targets, whereas both of the superresolution techniques easily resolve the targets and correctly locate their positions in range. In addition, the MLM algorithm (Fig. 5 (b)) correctly evaluates their power levels. As a matter of interest, these two targets were simulated on the basis of a "rotating object" [1] with a rotation rate of 0.1 rpm, so that decorrelation of the data samples from the two targets was achieved via a low doppler difference. This same two-target case was rerun with zero rotation (no doppler difference), but with the RF carrier subjected to frequency hopping over a one percent bandwidth in order to achieve decorrelation. The results were almost identical to Fig. 5 and, therefore, are not shown.

The final simulation for the quadriphase waveform involved a "rotating object" consisting of three 10 dB point-targets located at 14.3, 15.0, and 15.7, i.e., the targets are separated by 0.7 rangebins. Again, the rotaboom model [1] was rotated at a rate

of 0.1 rpm so that decorrelation was achieved via a low doppler difference. Figure 6 illustrates the performance results for the same three algorithms, and we note that this time performance is poor. The MLM algorithm does no better than the conventional matched filter, and although the eigenvector algorithm indicates three targets, the locations are not accurate. The technical reason for these poor results is that our quadriphase waveform of Fig. 2 only has two distinct phase slopes (degrees of freedom), such that it cannot handle three closely-spaced point targets.

CONCLUSIONS

Phase-coded waveforms have been investigated for compatibility with superresolution processing techniques, with the following results:

a) The bi-phase code waveform tested was not compatible and did not permit resolution finer than the conventional matched filter.

b) The quadriphase code waveform tested was partially compatible and permitted the resolution location of two point targets within the same rangebin. However, it could not handle more than two closely spaced targets because it is inherently limited to two degrees of freedom (for superresolution processing purposes).

It is concluded that phase-coded waveforms are not amenable to high resolution in the range domain. The extra burden of adding a processor to a typical radar system would not be cost effective in terms of the limited target resolution benefits available.

REFERENCES

1. W. F. Gabriel, "Superresolution Techniques and ISAR Imaging," NRL Memorandum Report 6714 published September 21, 1990.

2. D. L. Mensa, High Resolution Radar Imaging, Artech House, Dedham, MA 1982.

3. M. Skolnik (ed.), Radar Handbook, McGraw-Hill Book Co., NY, 1970.

4. R. H. Barker, "Group Synchronizing of Binary Digital Systems," in W. Jackson (ed.), "Communication Theory," pp. 273-287, Academic Press Inc., New York, 1953.

5. J. W. Taylor, Jr. and H. J. Blinchikoff, "The Quadriphase Code — A Radar Pulse Compression Signal and Unique Characteristics," Westinghouse Electric Corporation.

6. C. R. Vale, "SAW Quadriphase Code Generator," IEEE Trans. MTT, Vol. MTT-29, pp. 410-414, May 1981.

Appendix A

Waveform Signal Data Model

Consider a vector $\underline{E}(k)$ consisting of overlapping, noisy echoes of a radar signal with a apriori known phase/amplitude characteristics, where the index, k, denotes the k^{th} prf radar return. The elements of $\underline{E}(k)$ are the received complex signal data, sampled at precise intervals of time determined by the receiver bandwidth, B, i.e., the usual Nyquist sampling rate, f_s. The spacing of the data samples in the time domain is the reciprocal of f_s and defines a "rangebin" for the purposes of this discussion, i.e., the elements of $\underline{E}(k)$ represent precise data samples from adjacent rangebins. $\underline{E}(k)$ therefore represents a "range window" of data samples with a total of Q samples,

$$E(k)^t = [E_1(k),\ E_2(k),\ E_3(k),\ \ldots,\ E_q(k),\ \ldots,\ E_Q(k)] \qquad \text{(A1)}$$

where the index, q, denotes the q^{th} element/rangebin of $\underline{E}(k)$, and superscript, t, denotes the transpose of the vector.

The q^{th} data element, $E_q(k)$, consists of receiver noise plus a summation of overlapping echoes (if any) of our apriori known radar pulse compression waveform,

$$E_q(k) = \eta_q(k) + \sum_{i=1}^{I} p_i(k)\,\delta_{iq}\exp(\Psi_{iq}) \qquad \text{(A2)}$$

δ_{iq} = 0 for all q outside of the waveform echo.

δ_{iq} = 1 for all q inside of the waveform echo.

$\eta_q(k)$ is the k^{th} sample of independent Gausian receiver noise in the q^{th} rangebin; $p_i(k)$ is the k^{th} sample of the i^{th} echo complex multiplier referenced to the midpoint of the waveform; Ψ_{iq} is the sampled i^{th} waveform phase within the q^{th} rangebin referenced to the midpoint of the waveform; and I is the total number of echoes.

The waveform is assumed to be a pulse compression signal with a length of N rangebins, where N is usually significantly smaller than Q, such that any given waveform echo does not fill the range window represented by $\underline{E}(k)$. The position of the waveform echo depends upon the rangebin location of the i^{th} point-target, which is defined as the integer L_i,

$$L_i = INT(\tau_i + .5)$$
$$\text{where } \tau_i = \left(\frac{2r_i}{c}\right) \qquad \text{(A3)}$$

is the round trip time delay, r_i is the range of the i^{th} point-target within the range window, and c is the velocity of light. Our waveform echo can exist only over the region,

$$-\frac{N}{2} < (t_n - \tau_i) < +\frac{N}{2} \qquad 1 \le n \le N \qquad \text{(A4)}$$

where t_n is the n^{th} sampling time. The waveform index, n, is related to the range window index, q, via the range of the target,

$$q = n + L_i \qquad \text{(A5)}$$

It is often convenient to express the waveform sampling times, t_n, in terms of a symmetric integer form,

$$(t_n - \tau_i) = \frac{1}{2}(2n - N - 1) - (\tau_i - L_i) \qquad \text{(A6)}$$

where the term $(\tau_i - L_i)$, functions as a vernier shift for each of the N sampling times within the waveform. As an example, the phase function for a linear FM chirp waveform would be written [1],

$$\psi(t_n - \tau) = (\frac{\pi B}{N})(t_n - \tau)^2 \qquad \text{(A7)}$$

Therefore, the above relationships allow us to construct a convenient column vector in the form,

$$\underline{E}(k) = \underline{V}\underline{P}(k) + \underline{n}(k) \qquad \text{(A8)}$$

where $\underline{V}$ is a Q x I matrix containing a column vector, $\underline{v}_i$, for each of the I target waveform echoes. These column vectors are characterized by:

a) Zero elements except for the N values of index, q, associated with the waveform echo for the i^{th} target, equations (4) and (5). Note that targets in different rangebins will have some different values of the q index.

b) Very little change over typical observation times, such that the matrix $\underline{V}$ is not considered to be a function of the prf index, k. This is essential for separating out the basic variable of point-target range location.

$\underline{P}(k)$, on the other hand, is a column vector of I elements wherein the i^{th} element, $P_i(k)$, represents a complex multiplier for the waveform echo. It generally varies rapidly with time index, k, because it incorporates the phase term, $\omega_o \tau_i$, which is sensitive to target Doppler and RF carrier frequency shift. It's amplitude is dependant upon the target reflection coefficient. Phase variations in $P_i(k)$ are essential to achieving decorrelation of closely-spaced targets. Note that it is independent of the pulse compression waveform per se.

Proceeding then from equation (8), we can obtain the covariance matrix, $\underline{R}$, via application of the expected value operator, ξ, or ensemble average,

$$R = \xi[E(k)\,E^{\dagger}(k)] = \underline{V}\underline{P}\underline{V} + \sigma^2 I \tag{A9}$$

$$\text{where } \sigma^2 I = \xi[\underline{n}(k)\,\underline{n}^{\dagger}(k)] \tag{A10}$$

$$\text{and } P = \xi[\underline{P}(k)\,\underline{P}^{\dagger}(k)] \tag{A11}$$

where $\dagger$ is the conjugate transpose of the matrix. The diagonal elements of $\underline{P}$ represent the ensemble average power levels of the various target echoes, and off-diagonal elements can be non-zero if any correlation exists between the targets.

A true covariance matrix is never available, of course, so we average our data over K prf to obtain a sample covariance matrix, $\underline{R}$, and then proceed to compute near-optimum adaptive pulse compressing weighting, from which the target locations are estimated [1].

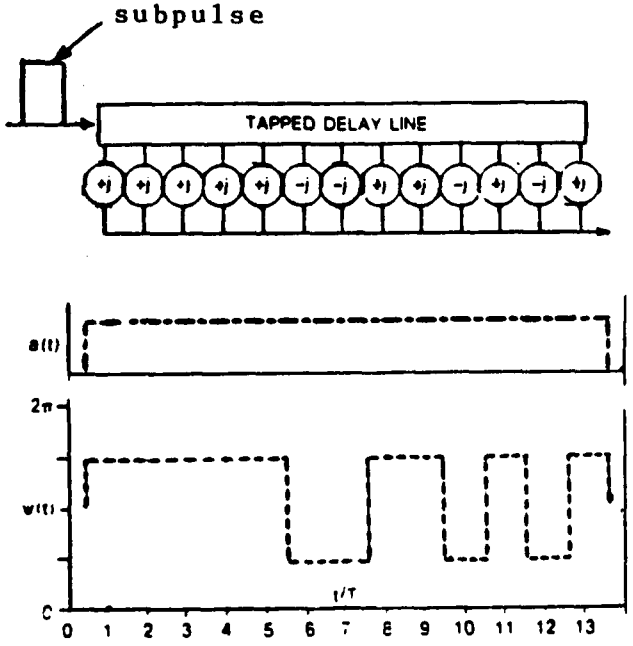

Fig. 1 - Generation of binary Barker code, N= 13.

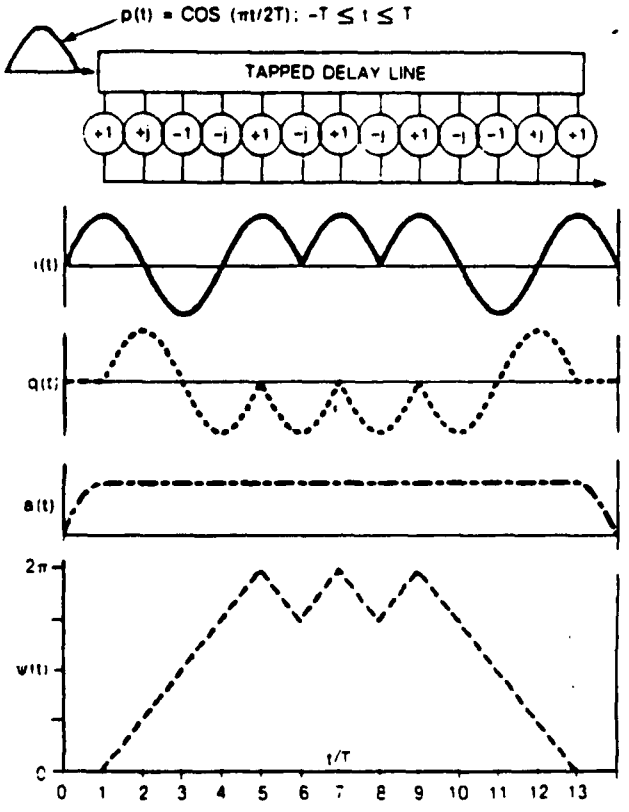

Fig. 2 - Generation of Quadriphase code, half-cosine pulse

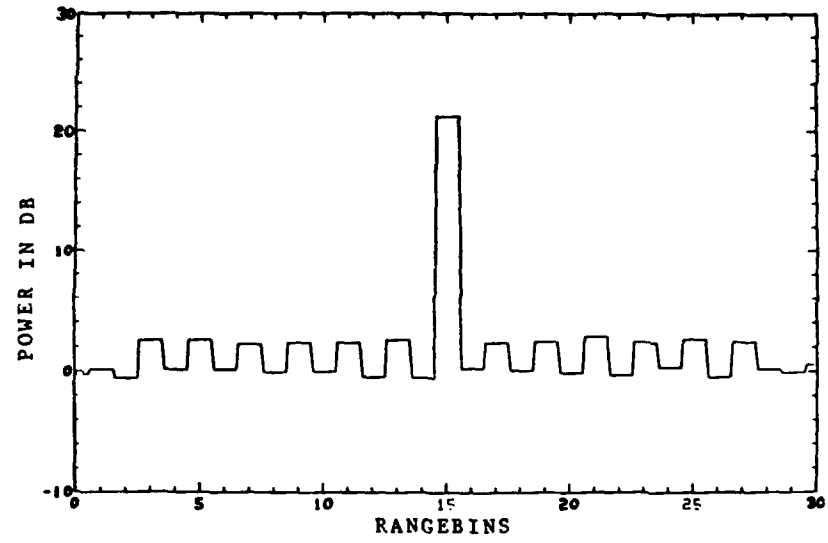

a) Fourier (matched filter response)

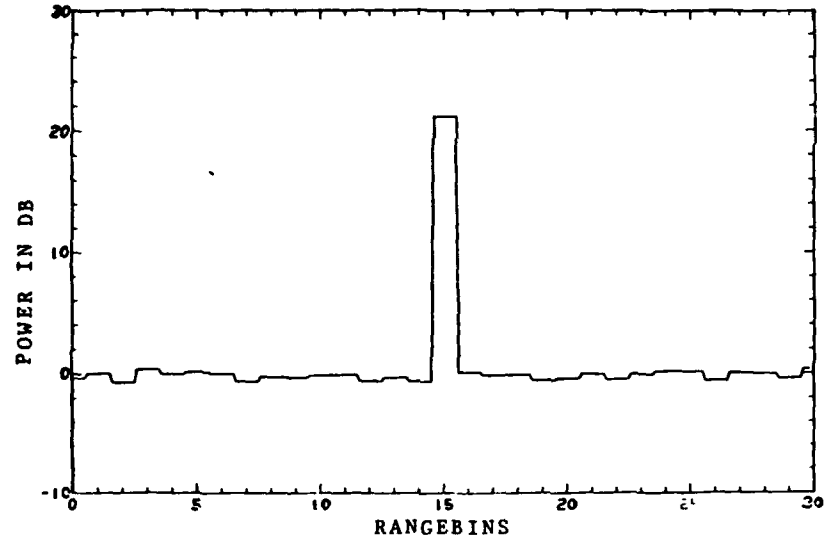

b) MLM algorithm

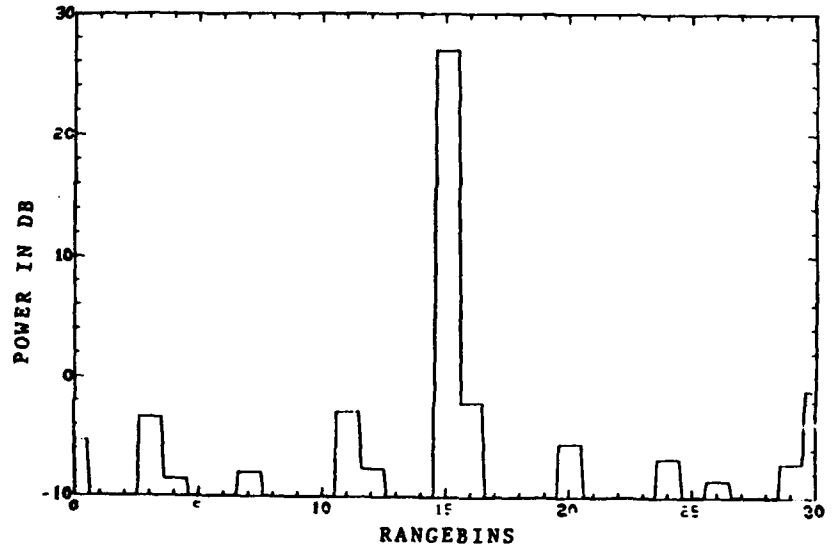

c) MUSIC Eigenvector algorithm

Fig. 3 - Range estimate plots using Bi-phase Code waveform, one 10 dB target located at 14.65, 264 prf processed.

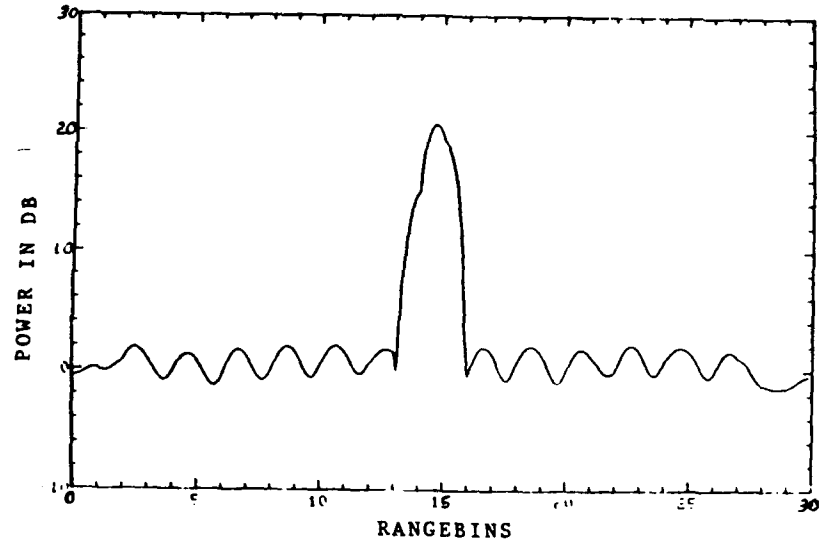

a) Fourier (matched filter response)

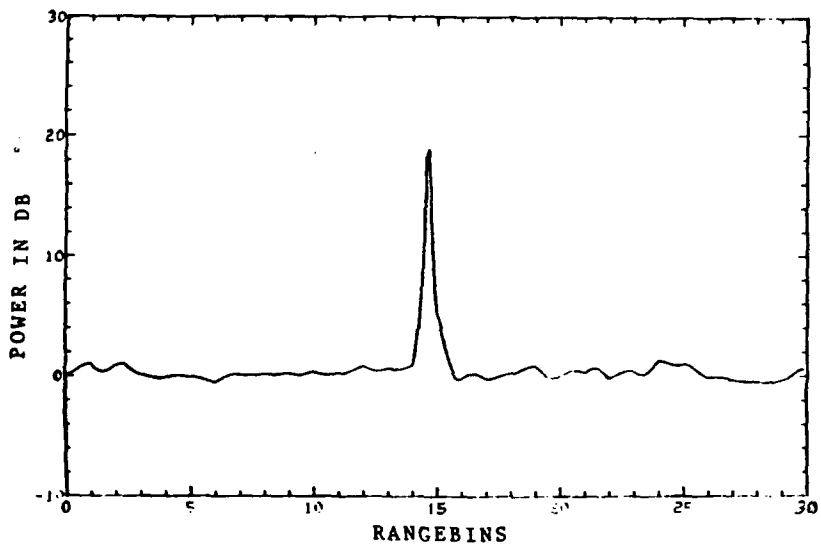

b) MLM algorithm

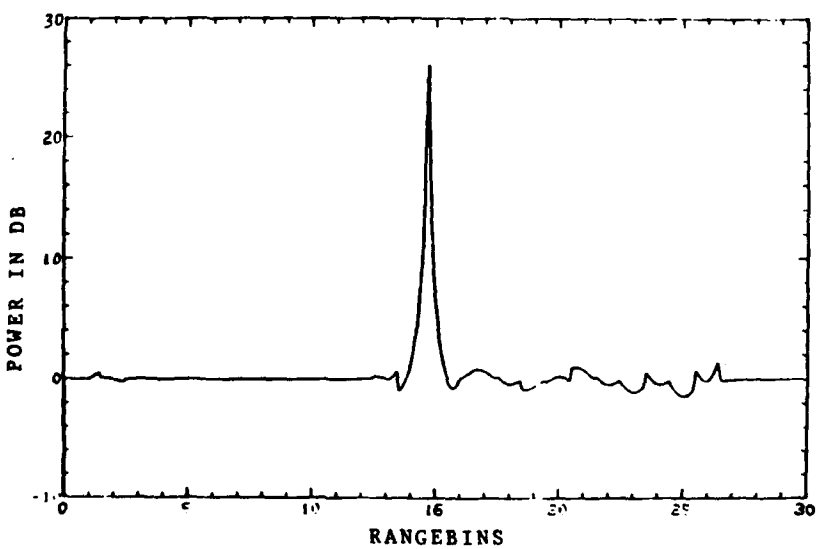

c) PEGS Eigenvector algorithm

Fig. 4 - Range estimate plots using Quadriphase Code Waveform, single target located at 14.65, 264 prf processed.

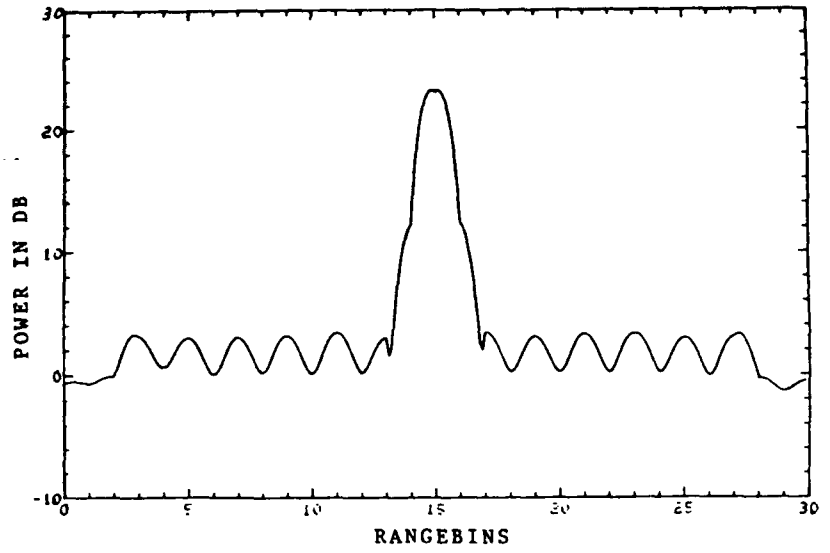

a) Fourier (matched filter response)

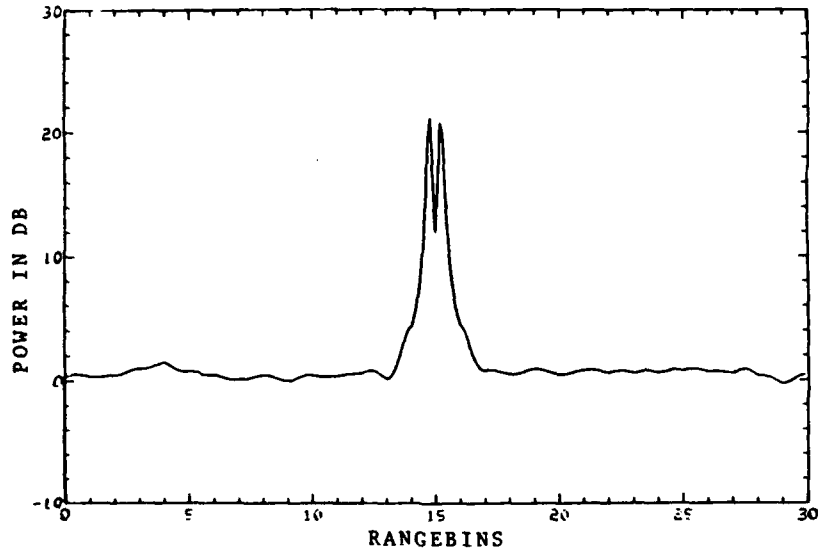

b) MLM algorithm

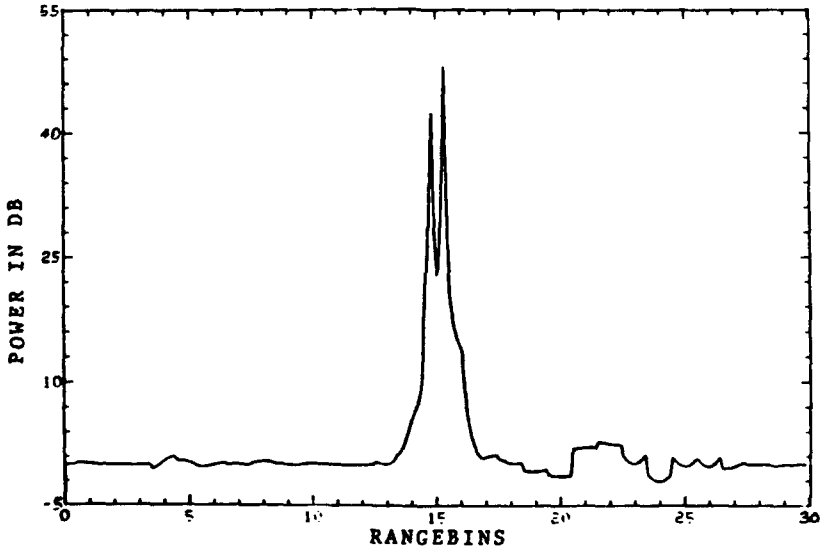

c) PEGS Eigenvector algorthm

Fig. 5 - Range estimate plots using Quadriphase Code Waveform, two targets located at 14.75 and 15.25 on Rotaboom, rotation rate 0.1 rpm, 264 prf processed.

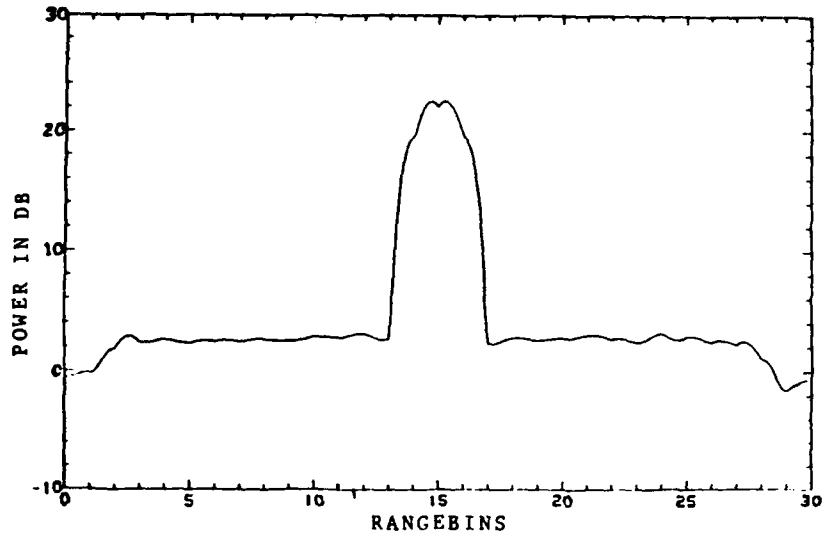

a) Fourier (matched filter response)

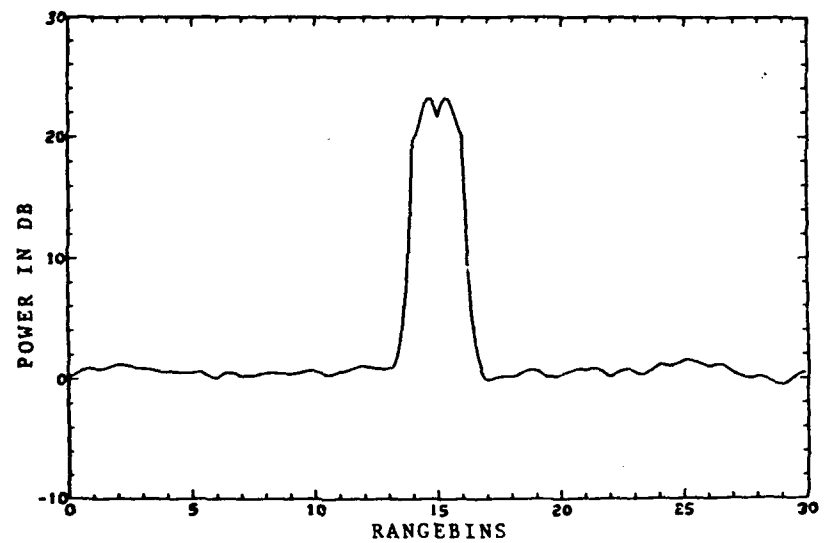

b) MLM Algorithm

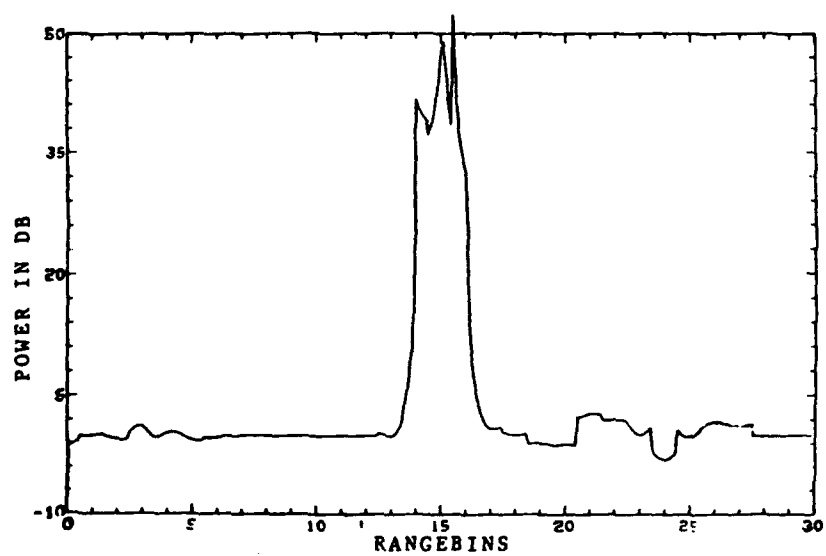

c) PEGS eigenvector algorithm

Fig. 6 - Range estimate plots using Quadriphase Code waveform, Three 10 dB targets located at 14.3, 15.0, and 15.7, rotaboom model, 264 prf processed.